JOURNAL OF Materials CHEMISTRY

Self propagating high-temperature synthesis of chromium substituted magnesium zinc ferrites $Mg_{0.5}Zn_{0.5}Fe_{2-x}Cr_xO_4$ ($0 \leqslant x \leqslant 1.5$)

Maxim V. Kuznetsov,[a] Quentin A. Pankhurst[a] and Ivan P. Parkin*[b]

[a] *Department of Physics and Astronomy, University College London, Gower Street, London, UK WC1E 6BT*
[b] *Department of Chemistry, University College London, 20 Gordon Street, London, UK WC1H 0AJ. E-mail: i.p.parkin@ucl.ac.uk*

Received 29th June 1998, Accepted 4th September 1998

Magnesium ferrite $MgFe_2O_4$ and chromium substituted magnesium–zinc ferrite $Mg_{0.5}Zn_{0.5}Fe_{2-x}Cr_xO_4$ ($0 \leqslant x \leqslant 1.5$) have been made in air by self-propagating high temperature synthesis (SHS), a combustion process involving the reaction of magnesium, zinc, iron(III) and chromium(III) oxides with iron or chromium metal powders and sodium perchlorate. This produced an orange–yellow propagation wave of velocity 2–3 mm s^{-1}. Two series of SHS samples were produced: series 1, SHS followed by annealing at 1400 °C for 2 h and series 2, SHS in a magnetic field of 1.1 T followed by annealing at 1400 °C for 2 h. X-Ray data showed that in all cases nearly phase pure cubic spinel ferrites were produced. Changes in the cubic lattice parameter were seen as a function of Zn and Cr content. Room temperature and 80 K Mössbauer data showed a significant change in sublattice occupancy with Cr content. Magnetic hysteresis data for series 1 and 2 showed that the coercive force of doped samples is higher than pure compositions whilst magnetisation is lower. It was also shown that the use of a magnetic field during SHS can influence the microstructure and magnetic properties of the final material.

Introduction

As part of an on-going research programme aimed at exploring the potentials and problems associated with innovative routes to ceramic materials, we are currently interested in synthesising materials by self-propagating high temperature synthesis (SHS).[1] This is a non-conventional method for materials synthesis which makes use of an exothermic chemical reaction. SHS processes rely on a balance between the heat generated and dissipated in a chemical reaction. It involves mixing different reactant powders, such as oxides, metals and non-metals, which on initiation produce an exothermic chemical reaction that is self-sustaining due to a positive energetic balance.[2] The reaction produces rapid heating (up to 3000 °C in 1–2 s) and cooling and is propagated by a combustion wave (also known as thermal flash, synthesis wave or solid flame) that moves out from the source of initiation. SHS processes are fast, do not require external energy such as from a furnace and can be used to produce complex oxides, intermetallics and composite materials. SHS reactions produce materials with unusual often porous microstructure.

Single phase magnesium ferrite $MgFe_2O_4$ with the spinel structure cannot be made from stoichiometric combination of MgO and Fe_2O_3. The spinel structure can be made by using a superstoichiometric amount of MgO (1.092 equivalents) to help combat oxygen loss from the ferrite.[3] Unsubstituted magnesium ferrites have low magnetic penetration and relatively small specific resistance. They have only limited industrial use. In contrast doped magnesium ferrite is known commercially as 'Ferramic-A' and has comparably good magnetic properties up to 100 MHz ($B_s = 1400$ G; $\rho = 4.5$ g cm^{-3}).[4] Much better properties are obtained for the series of solid solutions of Mg–Zn ferrite. The ferrite $Mg_{0.5}Zn_{0.5}Fe_2O_4$ is known commercially as Ferroxcube-2 and has a saturation magnetic induction $B_s = 3500$ G and a coercivity $H_c = 600$ G Oe^{-1} ($\rho = 4.7$ g cm^{-3}). These ferrites are used widely, for example in mobile telephones. Chromium substituted magnesium and magnesium–zinc ferrites are suitable not only for fundamental studies of structural and magnetic properties but also for industrial application. Chromium substituted iron ferrites of formula $MgFe_{2-x}Cr_xO_4$ are valuable for the long wave part of the high-frequency range (10–14 cm) as they have very low coefficient losses.[5] Pure and Cr-substituted Mg-ferrites also demonstrate catalytic activity.[6]

In this paper we present the first SHS preparation of chromium substituted Mg and Mg–Zn ferrites and investigate the effects of the presence of an applied magnetic field during the combustion synthesis.

Experimental

All reagents were obtained from Aldrich Chemical Company (UK) and used as supplied. Manipulations, weighings and grindings were performed under a nitrogen atmosphere in a Saffron Scientific glove box. SHS reactions were carried out in air on pre-ground powders on a ceramic tile using sodium perchlorate as an oxygen source. Initial reaction compositions are given in Table 1. The reactions were initiated by a heated filament (*ca.* 800 °C). Sintering was carried out in a Carbolite rapid heating furnace with heating and cooling rates of 20 °C min^{-1}. Samples were ground after the SHS reaction and also after sintering, and all measurements were recorded on powder samples. For the applied field SHS reactions a permanent magnet Halbach cylinder purchased from Magnetic Solutions Ltd was used. This 20 mm bore cylinder, comprising eight NdFeB magnets, provided a field of 1.1 T transverse to the cylinder axis. For the applied field SHS reactions a ceramic tile, containing the green mixture, was placed inside a quartz tube which was in turn inserted into the Halbach cylinder prior to initiation of the combustion process.

X-Ray diffraction was performed in reflection mode on a Philips X-Pert using unfiltered Cu-Kα radiation ($\lambda_1 = 1.5405$ Å, $\lambda_2 = 1.5443$ Å). Vibrating sample magnetometry was carried out on a Aerosonic 3001 magnetometer at room temperature in applied fields up to 7.5 kOe. ^{57}Fe Mössbauer spectra were recorded with a Wissel MR-260 constant acceleration spectrometer with a triangular drive waveform. Spectra were folded to remove baseline curvature and were calibrated relative to α-iron at room temperature. FTIR spectra were obtained as

Table 1 Molar ratio of components used in self-propagating high-temperature synthesis (SHS) of $Mg_{0.5}Zn_{0.5}Fe_{2-x}Cr_xO_4$, and nominal composition of the end product, using a notation where parentheses denote tetrahedral sites and square brackets denote octahedral sites

x	Fe_2O_3	Fe	Cr_2O_3	Nominal composition
0	0.50	1.00	0	$(Zn_{0.5}Fe_{0.5})[Mg_{0.5}Fe_{1.5}]O_4$
0.3	0.35	1.00	0.15	$(Zn_{0.5}Fe_{0.5})[Mg_{0.5}Fe_{1.2}Cr_{0.3}]O_4$
0.6	0.20	1.00	0.30	$(Zn_{0.5}Fe_{0.5})[Mg_{0.5}Fe_{0.9}Cr_{0.6}]O_4$
0.9	0.05	1.00	0.45	$(Zn_{0.5}Fe_{0.5})[Mg_{0.5}Fe_{0.6}Cr_{0.9}]O_4$
1.2	0.40	1.00 (Cr)	0.10	$(Zn_{0.5}Fe_{0.5})[Mg_{0.5}Fe_{0.3}Cr_{1.2}]O_4$
1.5	0.25	1.00 (Cr)	0.25	$(Zn_{0.5}Fe_{0.5})[Mg_{0.5}Cr_{1.5}]O_4$

KBr pellets on a Nicolet 205. SEM/EDAX measurements were performed using a Hitachi S570.

Preparation of $Mg_{0.5}Zn_{0.5}Fe_{2-x}Cr_xO_4$ ($0 \leqslant x \leqslant 1.5$)

The same reaction scale and procedure was used for all reactions illustrated here for $Mg_{0.5}Zn_{0.5}Fe_{1.4}Cr_{0.6}O_4$. Relative molar ratios of the reactants are given in Table 1.

Magnesium oxide (0.200 g, 5.0 mmol), iron oxide (0.638 g, 4 mmol), chromium oxide (0.916 g, 6 mmol), zinc oxide (0.204 g, 2.5 mmol), iron metal (1.116 g, 20 mmol) and sodium perchlorate (0.458 g, 3.75 mmol) were ground together in a pestle and mortar. The resultant solid was placed on a ceramic tile (*ca.* 1 cm by 7 cm strip) in air and a reaction initiated by means of a heated filament at one end. This produced an orange–yellow propagation wave of velocity *ca.* 2–3 mm s^{-1}. The resultant black powder was washed with distilled water (2×1 l) filtered through a Buchner funnel and air dried. The powder was reground and sintered at 1400 °C for 2 h. Yields in all reactions were essentially quantitative. The resultant powder was analysed by X-ray powder diffraction, Mössbauer spectroscopy, vibrating sample magnetometry, FTIR and SEM/EDAX.

Results

Sample preparation

SHS reactions were performed using various starting mixtures of Fe_2O_3, Fe, MgO, ZnO, Cr_2O_3 and $NaClO_4$. The molar ratio of each reagent was chosen to conform with the desired stoichiometry in the product, Table 1. At high degrees of chromium substitution ($Mg_{0.5}Zn_{0.5}Fe_{2-x}Cr_xO_4$; $x = 1.2$ and 1.5) Cr metal powder was used in the SHS process instead of Fe metal powder. The overall reaction is driven by the exothermic oxidation of Fe or Cr metal by oxygen which was evolved by the decomposition of sodium perchlorate at 600 °C.[7] In the case of $Mg_{0.5}Zn_{0.5}Fe_{1.7}Cr_{0.3}O_4$ the reaction scheme was:

$$0.5\ MgO + 0.5\ ZnO + 0.35\ Fe_2O_3 + 0.15\ Cr_2O_3 + Fe$$
$$+ 0.375\ NaClO_4 \rightarrow Mg_{0.5}Zn_{0.5}Fe_{1.7}Cr_{0.3}O_4 + 0.375\ NaCl$$

It should be noted that all reactions were carried out in air using solid oxidisers. Sodium perchlorate acts as the oxidising agent. On decomposition it co-produces sodium chloride which is easily removed from the product by washing with water.

The SHS preparation of pure and chromium substituted magnesium and magnesium–zinc ferrites is much quicker than standard conventional methods.[8,9] Using SHS instead of a furnace enables the first step in ferrite production to be reduced to *ca.* 30 s. In standard ceramic technology this stage requires some hours heating at 1200–1350 °C. The SHS reaction however does not completely alleviate the need to sinter the material. After the initial SHS reaction the product contained about 90% of the required ferrite mixed in with partially combined starting materials and sodium chloride. Subsequent washing with water followed by sintering of the powder at 1400 °C for 2 h produces virtually single phase ferrites. The sintering process is relatively quick as the SHS material has good contact between reacting grains.

Two different series of samples were prepared: series 1, the zero field SHS product subsequently sintered at 1400 °C for 2 h, and series 2, SHS product of an applied field synthesis of 1.1 T followed by sintering at 1400 °C for 2 h.

Characterisation

X-Ray powder diffraction showed that nearly single phase cubic spinel structures were produced for all the sintered products. Representative diffractograms are shown in Fig. 1, and the deduced lattice parameters are given in the Table 2. A

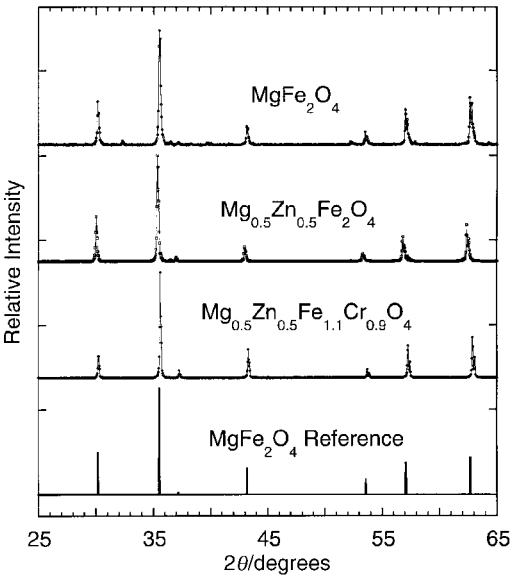

Fig. 1 Representative X-ray powder diffraction patterns obtained from the sintered products of the SHS reactions of: (1) MgO, Fe_2O_3, Fe and $NaClO_4$ in the ratio 1.00 : 0.50 : 1.00 : 0.375 to produce $MgFe_2O_4$; (2) MgO, ZnO, Fe_2O_3, Fe and $NaClO_4$ in the ratio 0.50 : 0.50 : 0.50 : 1.00 : 0.375 to produce $Mg_{0.5}Zn_{0.5}Fe_2O_4$, and (3) MgO, ZnO, Fe_2O_3, Fe, Cr_2O_3 and $NaClO_4$ in the ratio 0.50 : 0.50 : 0.50 : 1.00 : 0.45 : 0.375 to produce $Mg_{0.5}Zn_{0.5}Fe_{1.1}Cr_{0.9}O_4$. Also shown for comparison is a reference stick pattern for $MgFe_2O_4$.

Table 2 Cubic lattice parameter a for two series of $MgFe_2O_4$ and $Mg_{0.5}Zn_{0.5}Fe_{2-x}Cr_xO_4$ samples produced by self-propagating high-temperature synthesis (SHS): series 1, zero field SHS followed by annealing at 1400 °C for 2 h; series 2, SHS conducted in a magnetic field of 1.1 T followed by annealing at 1400 °C for 2 h

$Mg_{0.5}Zn_{0.5}Fe_{2-x}Cr_xO_4$ x	a^a/Å	
	Series 1	Series 2
0	8.416	8.415
0.3	8.408	8.399
0.6	8.398	8.379
0.9	8.375	8.369
1.2	8.373	8.367
1.5	8.362	8.334
$MgFe_2O_4$	8.381	8.377

[a]Error limit: ±0.004 Å.

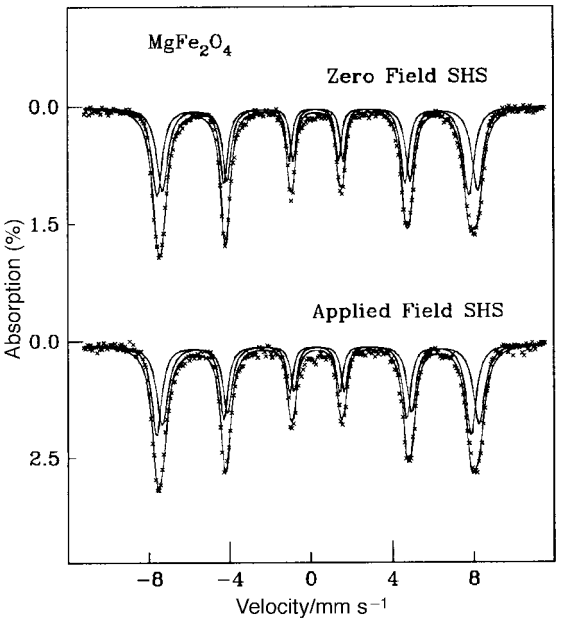

Fig. 2 Room temperature Mössbauer spectra for samples of $MgFe_2O_4$ prepared by SHS in zero field and in a field of 1.1 T, after sintering for 2 h at 1400 °C. Solid lines represent a least squares fit with two subcomponents corresponding to Fe atoms in octahedral and tetrahedral sites in the spinel structure.

general decrease in *a* parameter with increasing chromium content was noted. This mirrors the same results for conventionally prepared materials.[10,11] This variation in unit cell may be attributed to the smaller ionic radii of six-coordinate Cr^{3+} ions compared to those of six-coordinate high spin Fe^{3+} ions.[12] The chromium preferentially replaces iron from octahedral sites because of favourable crystal field effects (Cr^{3+} 6/5 Δ_o, Fe^{3+} 0 Δ_o).

For series 1 materials the lattice parameters were consistently larger than for series 2, albeit at the limits of experimental resolution. This effect is minor, and might be explained by differences in the degree of Cr substitution achieved in the two series. However, from our observations both series of products appear to be almost single phase, with no signs of unreacted chromium oxide. We surmise therefore that this observation may be an effect of the applied field during synthesis.

EDAX measurements for $Mg_{0.5}Zn_{0.5}Fe_{2-x}Cr_xO_4$ showed the presence of magnesium, iron, chromium and zinc only (oxygen was below the machine cut off). The elemental ratios were within experimental error (1–2%) identical for the same sample across many surface spots indicating that a homogeneous powder was formed. The atom percentages mirrored very closely the expected values, for example the sample of formula $Mg_{0.5}Zn_{0.5}Fe_{0.5}Cr_{1.5}O_4$ gave an average elemental ratio of $Mg_{0.5}Zn_{0.5}Fe_{0.6}Cr_{1.6}$.

The FTIR spectra of $MgFe_2O_4$ and $Mg_{0.5}Zn_{0.5}Fe_{2-x}Cr_xO_4$ mirrored previous literature measurements, showing three broad overlapping bands: a shoulder at 685 cm^{-1} and two bands at 520 and 410 cm^{-1}. An additional band grows into the spectra at 620 cm^{-1} with increasing chromium substitution. The absorption bands are all characteristic of metal oxygen stretches.

^{57}Fe Mössbauer absorption spectra were recorded for series 1 and 2 samples of $MgFe_2O_4$ at room temperature (see Fig. 2), and of $Mg_{0.5}Zn_{0.5}Fe_{2-x}Cr_xO_4$ at room temperature and at 80 K (see Fig. 3). The spectra were least squares fitted using Lorentzian lineshapes and a first order perturbation approach to the combination of electric quadrupole and magnetic interactions. For the $MgFe_2O_4$ samples two subcomponent spectra, attributable to Fe atoms in the octahedral and tetrahedral sites, were fitted. For the $Mg_{0.5}Zn_{0.5}Fe_{2-x}Cr_xO_4$ spectra broad lines were observed, indicating the occurrence of distributions in the environments of the ^{57}Fe nuclei, with corresponding distributions in the Mössbauer hyperfine parameter. Such distributions are to be expected in the chromium substituted materials where the Cr atoms disrupt the long range magnetic interactions between the Fe atoms. Consequently these spectra were analysed using a 200 box histogram model for the distribution of hyperfine fields experienced by the ^{57}Fe nuclei. For simplicity a single isomer shift parameter was used for all the histogram subspectra, and the quadrupole splitting was set to zero. The linewidths of the histogram subspectra were fixed at an appropriate experimental minimum, namely 0.28 mm s^{-1}. Smoothing and endpoint constraints were applied to the allowed histogram solutions. Further details of the histogram fitting program are available elsewhere.[13] The fitted spectra are shown as solid lines in Fig. 2 and 3 and selected parameters obtained from these fits are given in Table 3 and 4.

Hysteresis loops were recorded on all the samples in fields up to 7.5 kOe at room temperature. Representative data are shown in Fig. 4. The maximum magnetisation σ_{max}, remanent magnetisation σ_r and coercive force H_c are listed in Table 5. For all samples prepared in magnetic field (series 2) the magnetic parameters are greater than those prepared in the absence of a magnetic field. A general decrease in σ_{max} and σ_r and an increase in H_c was observed with chromium substitution.

Discussion

Mössbauer measurements

It is well known that magnesium ferrite $MgFe_2O_4$ has an inverse spinel structure with Mg occupying octahedral sites and Fe equally occupying octahedral and tetrahedral sites: $Fe[MgFe]O_4$. In contrast zinc ferrite is a normal spinel with Zn occupying the tetrahedral positions and Fe occupying the octahedral sites: $Zn[Fe_2]O_4$. Mg–Zn ferrite is a solid solution between these, with Zn^{2+} ions occupying tetrahedral sites and Mg^{2+} ions on octahedral sites. Chromium substitution into this species occurs preferentially on the octahedral sites.

From the current set of Mössbauer spectra these site occupancies may be tested for the pure Mg ferrites, as shown in Fig. 2. As can be seen from the data, reasonable quality fits have been obtained for both the zero field and applied field SHS samples assuming an equal spectral area for the two

Table 3 Room temperature Mössbauer parameters for sintered $MgFe_2O_4$ ferrites prepared *via* SHS reactions performed in zero field and in an applied field of 1.1 T (series 1 and 2): isomer shift δ ($\pm$0.01 mm s^{-1}); quadrupole shift 2ε ($\pm$0.01 mm s^{-1}); linewidths Γ and $\Delta\Gamma$ ($\pm$0.01 mm s^{-1}) and hyperfine field B_{hf} ($\pm$0.1 T). Two equal area subspectra were fitted, corresponding to Fe atoms at the octahedral and tetrahedral sites. Preferential line broadening due to distributions in local environments was modelled by ascribing linewidths of $\Gamma+\Delta\Gamma$, Γ and $\Gamma-\Delta\Gamma$ to the outer, middle and inner pairs of lines in the sextets

	Octahedral sextet					Tetrahedral sextet				
	δ	2ε	Γ	$\Delta\Gamma$	B_{hf}	δ	2ε	Γ	$\Delta\Gamma$	B_{hf}
Series 1	0.43	0.06	0.51	0.16	48.1	0.16	−0.08	0.49	0.14	47.6
Series 2	0.45	0.04	0.54	0.15	48.3	0.17	−0.08	0.49	0.11	47.9

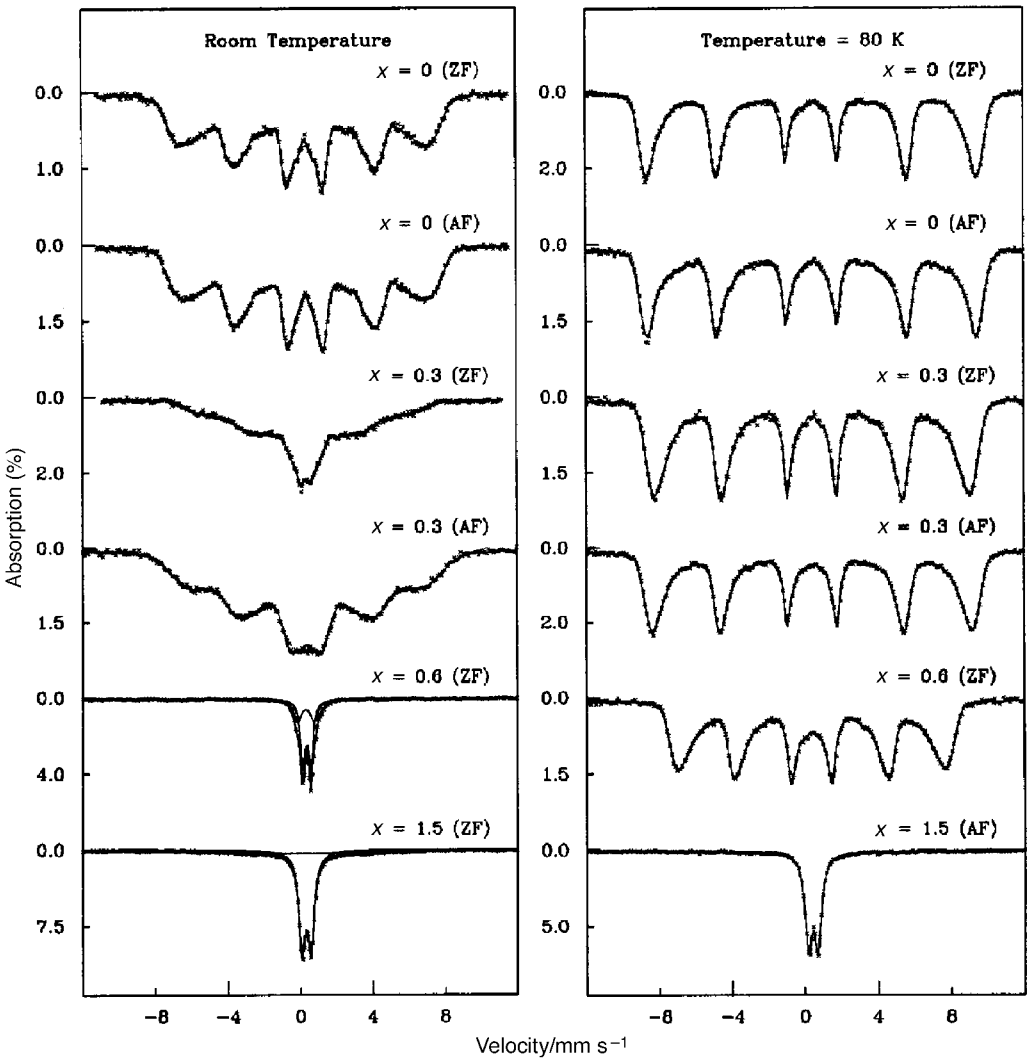

Fig. 3 Mössbauer spectra measured at room temperature and at 80 K for samples of $Mg_{0.5}Zn_{0.5}Fe_{2-x}Cr_xO_4$ ($x=0$, 0.3 and 0.6) prepared by SHS in zero field and in an applied field of 1.1 T, after sintering for 2 h at 1400 °C. Solid lines represent least squares fits to the data: for the magnetically split spectra a probability distribution of hyperfine fields was used, otherwise a combination of one or two quadrupole split doublets was used.

subcomponent sextets. This is consistent with the equal occupancy of octahedral and tetrahedral sites by the Fe atoms. The parameters obtained from the fits, given in Table 3, are also consistent with this assignment. Comparison of the Mössbauer parameters for the two samples shows only minor differences, although it may be significant that the hyperfine fields at both the octahedral and tetrahedral sites in the applied field SHS sample are larger than in the zero field SHS counterpart.

Mössbauer spectra of some selected $Mg_{0.5}Zn_{0.5}Fe_{2-x}Cr_xO_4$ samples recorded at room temperature and 80 K are shown in Fig. 3. We note in passing that further Mössbauer experiments, such as at liquid helium temperatures in the presence of large external magnetic fields, could be used to garner information

Table 4 Mössbauer parameters at room temperature and 80 K for selected examples of sintered $Mg_{0.5}Zn_{0.5}Fe_{2-x}Cr_xO_4$ ferrites prepared *via* SHS reactions in zero field and in an applied field of 1.1 T (series 1 and 2): isomer shift δ (±0.01 mm s^{-1}) and mean hyperfine field $\langle B_{hf}\rangle$ (±0.5 T). The spectra were modelled with a 200 box histogram probability distribution of subcomponent sextets, each of which had the same isomer shift δ, a quadruple shift of zero, and a hyperfine field covering the range from zero to 65.0 T. In some cases the spectra comprised one or two paramagnetic doublets, in which case the parameters given are the isomer shift δ (±0.01 mm s^{-1}) and quadrupole splitting Δ (±0.01 mm s^{-1})

	Room temperature spectra						Spectra at 80 K					
	Series 1			Series 2			Series 1			Series 2		
x	δ	Δ	$\langle B_{hf}\rangle$	δ	Δ	$\langle B_{hf}\rangle$	δ	Δ	$\langle B_{hf}\rangle$	δ	Δ	$\langle B_{hf}\rangle$
0.0	0.32	—	31.7	0.33	—	31.4	0.43	—	49.9	0.42	—	48.0
0.3	0.33	—	19.7	0.35	—	27.4	0.42	—	46.1	0.42	—	47.2
0.6	0.31	0.90	—				0.38	—	36.5			
	0.35	0.42	—									
1.5	0.33	0.49	—				0.44	0.52	—			

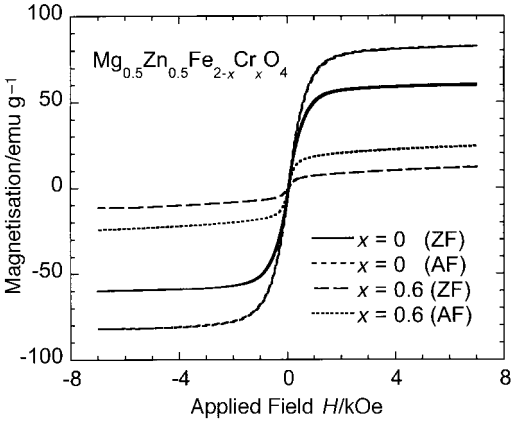

Fig. 4 Representative room temperature hysteresis loops of samples of $Mg_{0.5}Zn_{0.5}Fe_{2-x}Cr_xO_4$ prepared by SHS in zero field (ZF) and in an applied field (AF) of 1.1 T, after sintering at 1400 °C for 2 h.

Table 5 Bulk magnetic properties of sintered $MgFe_2O_4$ and $Mg_{0.5}Zn_{0.5}Fe_{2-x}Cr_xO_4$ prepared by SHS performed in zero field and in an applied field of 1.1 T (series 1 and 2): maximum magnetisation σ_{max} ($\pm$0.1 emu g^{-1}), remanent magnetisation σ_r ($\pm$0.1 emu g^{-1}) and coercive force H_c ($\pm$0.5 Oe). Measurements were made at room temperature in applied fields up to 7.5 kOe

$Mg_{0.5}Zn_{0.5}Fe_{2-x}Cr_xO_4$	Series 1			Series 2		
x	σ_s	σ_r	H_c	σ_s	σ_r	H_c
0	59.8	1.42	9.4	82.6	1.80	9.3
0.3	46.8	1.34	9.9	59.1	1.37	9.8
0.6	12.2	0.31	12.5	24.5	1.10	11.8
0.9	2.45	0.19	16.7	10.9	0.56	16.2
1.2	0.99	0.14	39.5	2.78	0.26	21.7
1.5	0.61	0.10	82.0	1.17	0.24	77.4
$MgFe_2O_4$	34.6	1.97	19.8	39.6	2.42	18.3

on the cation distributions in the Cr substituted materials.[14] However, in the present work we choose to limit our consideration to the general features of the Mössbauer spectra of these samples, and to a comparison of the data obtained from the series 1 and 2 samples.

On inspection of Fig. 3 it is apparent that in the case of $Mg_{0.5}Zn_{0.5}Fe_2O_4$ there is little difference between the series 1 and 2 samples either at room temperature or at 80 K, while there are discernible differences between the two series for $Mg_{0.5}Zn_{0.5}Fe_{1.7}Cr_{0.3}O_4$ at room temperature, but less so at 80 K. The fitted parameters in Table 4 bear this out, with the main difference being a higher mean hyperfine field in the applied field SHS $x=0.3$ sample at room temperature than in its zero field counterpart. We tentatively ascribe this to a possibly less disruptive distribution of substituted Cr atoms in the series 2 sample, with a commensurate increase in the samples Curie temperature. However, such a result needs further investigation, beyond the scope of the present study, before this can be known for certain, especially since a slightly different level of Cr doping in the two samples might give rise to a similar effect.

Representative data for the higher Cr dopings of $x=0.6$ and 1.5 are also shown in Fig. 3 for series 1 samples. These spectra are paramagnetic doublets at room temperature, indicating that in these samples the Cr substitution is sufficiently high to disrupt the Fe ordering enough that the Curie temperatures of the samples fall below room temperature. Indeed, for the $x=1.5$ sample the Curie temperature falls below 80 K, so that even at that temperature a doublet is measured. For the $x=0.6$ sample at 80 K a broad hyperfine split spectrum is observed, with parameters that are in line with those seen for the lower Cr content samples.

Magnetic measurements

As is evident from the data in Table 5, the introduction of Cr^{3+} ions into magnesium zinc ferrite strongly affects the room temperature magnetic parameters of the system. The decrease in both the maximum magnetisation σ_{max} and the remanent magnetisation σ_r mirrors the fall in Mössbauer hyperfine fields, and may be ascribed to the increasing fluctuations in the Fe moments as the increasing Cr concentration disrupts the interatomic exchange interactions. Systematic differences in the magnetisation parameters are seen for the series 1 and 2 samples, with the applied field samples having consistently higher σ_{max} and σ_r parameters. This is most probably indicative of a degree of magnetic texturing, generated during the applied field SHS processing, remaining in the sintered powders. This is an interesting result and indicative of possible microstructural effects which may be related to the lattice parameter changes seen earlier in the X-ray diffraction experiments. In contrast the coercive force H_c data for both series 1 and series 2 samples are similar.

Effect of magnetic field on the synthesis

The only difference between the samples prepared in series 1 and 2 was the application of an external magnetic field during the SHS step. Despite this, the two series of samples show some small differences in X-ray and Mössbauer parameters, and major differences in magnetic parameters. The changes in unit cell dimension may indicate different levels of cross-substitution or defects in the two series. These effects may have arisen as a consequence of a slightly faster propagation rate, coupled with an increased reaction temperature, in the applied field SHS reactions: visual inspection of the reactions indicated that the synthesis wave moved faster and glowed with a more yellow coloration in the applied field series. In the applied field some pre-organisation of the precursor powders was observed prior to initiation of the SHS reaction, most likely due to the alignment of the iron and iron oxide components along the magnetic flux lines. It is reasonable to suppose that this pre-organisation leads to better surface contacts between the reacting powders, hence giving rise to the hotter and faster reaction conditions.

Conclusions

Self propagating high temperature synthesis allows the rapid formation of near single phase chromium substituted magnesium and magnesium zinc ferrite. Despite the short synthesis time solid solutions of the ferrites were formed. The ferrites had magnetic orders of merit equal to those prepared by conventional synthesis. Mössbauer spectroscopy showed that for all samples the chromium metal was substituted on the octahedral sites within the spinel. Use of a magnetic field during SHS synthesis increases the rate of reaction propagation. The materials prepared by SHS in a magnetic field showed increased saturation magnetisation compared to those prepared in the absence of a field. It is likely that these enhanced magnetic effects are a consequence of changes in product microstructure rather than in spinel site occupancy.

References

1 I. P. Parkin, *Chem. Soc. Rev.*, 1996, 199; I. P. Parkin, G. E. Elwin, A. V. Komarov, Q. T. Bui, Q. A. Pankhurst, L. Fernandez Barquin and Y. G. Morozov, *J. Mater. Chem.*, 1998, **8**, 573.
2 A. G. Merzhanov, *Proc. Technol.*, 1996, **56**, 222.
3 A. E. Padalino, *J. Am. Ceram. Soc.*, 1960, **43**, 183; Y. D. Tretyakov and N. I. Oleinikov, *Inorg. Mater.*, 1965, **1**, 254.
4 Ferrites, ed. L. A. Rabkin, S. A. Soskin and B. S. Epshtein, Energy, Leningrad, 1968, p. 384.
5 H. Kojima, in *Ferromagnetic Materials*: *A Handbook of the*

Properties of Magnetically Ordered Substances, ed. E. P. Wohlfarth, North-Holland, Amsterdam, 1982, vol. 3.
6 V. S. Darshane, S. S. Lokegaonkar and S. G. Oak, *J. Phys. IV Fr.*, 1997, **7**, C1.
7 M. V. Kuznetsov, Y. G. Morozov, M. D. Nersesyan and T. I. Ignateva, *Inorg. Mater.*, 1995, **31**, 1125.
8 L. C. F. Blackman, *Trans. Faraday Soc*., 1959, **55**, 391.
9 A. H. Morrish and P. E. Clark, *Phys. Rev. B*, 1975, **11**, 278.
10 E. W. Gorter, *Philips Res. Rep*., 1954, **9**, 295.
11 F. C. Romeijn, *Philips Res. Rep.*, 1953, **8**, 304.
12 R. Shanon, *Acta Crystallogr.*, *Sect. A*, 1976, **32**, 751.
13 Q. A. Pankhurst, S. Suharan and M. F. Thomas, *J. Phys. Condens. Matter*, 1992, **4**, 3551.
14 P. M. A. de Bakker, E. De Grave, D. Gryffroy, R. E. Vandenberghe and P. Moens, *Mater. Sci. Forum*, 1991, **79–82**, 777.

Paper 8/04942D